# Different UV-B Exposure Times Induce Phenotypic, Transcriptomic, and Proteomic Changes in Wine Grape Leaves

**Su Li** ( 76353567@qq.com )

School of Plant Protection, Yunan Agricultural University, Kunming, P.R.China. 650201.

https://orcid.org/0000-0003-1018-2736

**Zhao Yue**

Yunnan Agricultural University

**Sun Qingyang**

Yunnan Agricultural University

**Zhu Yifan**

Yunnan Agricultural University

**Research article**

**Keywords:** UV-B irradiation, wine grape, leaf epidermis, palisade tissue, proteome, transcriptome

**Posted Date:** October 19th, 2020

**DOI:** https://doi.org/10.21203/rs.3.rs-92699/v1

# Abstract

[Background]The *Cabernet Sauvignon* grape, considered “the world's most renowned grape variety for the production of fine red wine”, is cultivated in many regions, such as the plateau area in Shangri-La, southwest China. This area is characterized by dry and strong UV climate owing to a high altitude. Previous studies have shown that UV radiation, especially UV-B, improves plant resistance to cold, disease and dry circumstance. In fact, the *Cabernet sauvignon*, mainly grown in Shangri-La where the UV intensity reaches 21-22w/$m^2$, has shown strong resistance in the past decades.

[Aims] However, UV-B’s effect Cabernet Sauvignon grape leaves remains unknown. As a result, we would like to explore the effects of UVB on grape leaves at high altitude through experiments. [Methods]In the present study, we investigated anatomical changes, and photosynthetic changes in *Cabernet Sauvignon* plants and analyzed transcriptomic and proteomic regulation of these changes following exposure to 15-20w/$m^2$ UV-B for 3 and 7 days.

[Results]Results revealed that UV-B exceeding 10w/$m^2$ could change morphology and arrangement of epidermal and palisade tissue cells. We also found upregulation of proteins that regulate cytoskeletal and cell wall synthesis, after 3 days of exposure to UV-B. On the other hand, proteins associated with disease-resistance and antioxidants were up-regulated after 7 days of exposure. Transcriptomic results revealed enrichment of both proteins and genes associated with pathogen infection, defense and antioxidant processes.

[Conclusion]As a result, the study showed that strong UV radiation at high altitude did contribute to increased disease resistance and environmental adaptability of grape plants.


# Introduction

Ultraviolet rays have different effects on plant growth processes including photosynthesis [1], flavonoid synthesis [2], protein metabolism [3], physiological and biochemical processes [4–8]. Specifically,UV-B has been previously implicated in a reduction in plant height, leaf area and dry fresh weight of aboveground and underground parts in some species [9]. Similarly, synthesis of ultraviolet-resistant pigments, that absorb UV rays and protect DNA from light damage, was reportedly enriched following exposure to ultraviolet [10]. Additionally, previous studies have shown that UV-B inhibits plant photosynthesis, thereby causing a decline in total chlorophyll content. Consequently, the resulting photosynthetic products are restrained compared to those from unirradiated plants, causing failure of the entire photosynthetic system and stomatal sensitivity [11]. Moreover, short-wave ultraviolet radiation, like UVC, has been shown to compromise plant resistance to diseases [12]. Generally, previous studies have mainly focused on UV-induced changes and metabolism, but not changes in leaf structure.

Shangri-La is a wine-growing region characterized by low latitude and high altitude. The *Cabernet Sauvignon* grape is planted at attitudes ranging from 1850 to 2800 m. However, its yield and quality, at

attitudes above 2200 m, are significantly affected by ultraviolet radiation, which reaches 15-20w/$m^2$ at daytime[12]. Consequently, this effect in quality has been implicated in poor flavor of the wine. In the present study, we analyzed structural leaf changes in *Cabernet Sauvignon* plants following UV exposure, to understand morphological changes in epidermal cells and palisade tissues, as well as ascertain cellular responses to UV-B.

# Results

## UV-B induces phenotypic and structural changes in the leaf epidermis

When exposed to 15-20w/$m^2$ UV-B for 3 days, leaves that were 15 cm away from the lamp stopped growing both horizontally and longitudinally. Those exposed for 7 days exhibited brown spots and suspected burn marks on leaf surfaces, whereas their edges were slightly curled (Fig.1a). Damage and discoloration were evident on both new and developing leaves, compared with those of untreated. Cells in the upper epidermis as well as those in the palisade tissue were compressed. In addition, a narrow cell width and a shorter intercellular space were evident, when exposure time was increased from 3 to 7 days (Fig. 1b).

## Statistical results

## UV-B induces changes in cell density and morphology

Statistical results revealed a time-dependent increase in the number of cells per unit area as well as the morphology of cells. For example, at 7 days post exposure, longer palisade tissue cells were observed in plants exposed to 15-20w/m2 UV-B, relative to those in the other two treatments. Conversely, the upper epidermal cells were shorter at 7 days of exposure, relative to the other two treatments (Fig. 2).

### UV-B induces change of photosynthesis

Parameters related to photosynthesis, including leaf temperature, net photosynthetic rate (Pn), intercellular carbon dioxide concentration (Ci), stomatal conductance (Gs) and transpiration rate (Tr), were simultaneously measured using the GFS3000 photosynthetic analyzer (Germany). Results showed that leaf temperature and net photosynthetic rate at 3 and 7 days post exposure were not significantly different from those of the CK group. Conversely, intercellular carbon dioxide concentration, stomatal conductance and the transpiration rate significantly increased with exposure time (Fig. 3).

### Proteomic and transcriptomic results following exposure to UV-B

### Levels of CK protein expression across exposure times

Results from proteomics analysis revealed that 142 proteins were differentially expressed at 3 days post exposure. Specifically, 123 and 19 were up- and downregulated, respectively. 7 days post exposure, 188 proteins were differentially expressed, relative to those in the CK treatment. Among them, 132 and 56

proteins were up- and down-regulated, respectively. In addition, 90 proteins were significantly enriched at both exposure times, among which 42 and 49 were up- and down-regulated, respectively (Table1).

GO results revealed that transcripts were exclusively enriched at the chromatin remodeling and oxidoreductase activity levels. Specifically, DNA replication-independent nucleosome assembly and chromatin remodeling at centromere were for the key processes enriched at 3 days post UV-B exposure (FDR<0.05) (Table 3). On the other hand, glyoxylate metabolic activity was overexpressed in samples at 7 , relative to those at 3 days post exposure. In total, 17genes were consistently down-regulated in binding activities. Additionally, KEGG analysis revealed the most significant signal transduction pathways, including those involved in biosynthesis and metabolism (Table 2). Furthermore, a scatter plot of these results showed enrichment in the ratio of the rich factor, known as the number of different and annotated genes, across the endoplasmic reticulum, secondary metabolism, and plant hormone signal transduction (Appendix A).

**Table1.** Profiles of protein expression following UV-B exposure

| Pair comparison | No. of Common proteins | No. of differential proteins | No. of Significant Up-regulated proteins | No. of Significant down-regulated proteins |
|---|---|---|---|---|
| 3-day vs 0day | 6410 | 142 | 123 | 19 |
| 7-day vs 0day | 6396 | 188 | 132 | 56 |
| 3-day vs 7-day | 6417 | 90 | 42 | 49 |

**Table 2.** Profiles of protein expression following a group comparison

| Pair comparison | Number of differential expressed genes | Up-regulated genes | Down-regulated genes |
|---|---|---|---|
| 3-day vs 0day | 176 | 96 | 80 |
| 7-day vs 0day | 477 | 343 | 134 |
| 3-day vs 7-day | 79 | 65 | 14 |

In the hierarchical clustering diagram, the log10 (FPKM+1) value was normalized (scale number) and clustering was conducted. Red and green represent up-and down-regulated genes, respectively.

### UV-B induces protein expression and pathways associated with cell morphology

Exposure of grape leaves to 15-20w/$m^2$ UV-B, for 3 days, resulted in upregulation of proteins associated with cell wall synthesis and cell morphological (Table 3). This indicated that UV-B induces changes in cell morphology, arrangement of epidermal and palisade cells in the leaves, resulting in thickening of the epidermis. KEGG analysis revealed high enrichment of metabolic pathways related to morphology and arrangement of epidermal cells, including the isoquinoline alkaloid, tropane, pyridine and piperidine synthesis pathways. Among these pathways, the intermediate G type of serine/threonine protein kinase and the amine oxidase were upregulated, resulting in changes in epidermal cells. Additionally, alpha and beta type tubulin were significantly upregulated, causing changes in the intercellular space (Fig. 4).

**Table 3**. Expression profiles of cell morphology-related proteins induced by UV-B

| Pair comparison | Protein ID | Description | P-value |
|---|---|---|---|
| 3-day vs CK | XP_002274910.2 | the Receptor protein kinase TMK1 | 0.0174521 |
| 7-day vs CK | NP_001267891.1 | basic endochitinase precursor [Vitis vinifera] | 0.0023727 |
| 3-day vs 7-day | XP_010646925 | probable xyloglucan endotransglucosylase/hydrolase protein 7 | 0.0014167 |
| | NP_001290017 | the lipoxygenase | 0.0046262 |
| | XP_002268404.1 | probable carotenoid cleavage dioxygenase 4, chloroplastic [Vitis vinifera] | 0.0026872 |
| | NP_001268208 | the cell wall apoplastic invertase | 0.0010424 |
| | NP_001268052 | ripening-related protein grip22 precursor [Vitis vinifera] | 0.0247628 |
| | | | 0.0024165 |
| | | | 0.0032486 |

### UV-B mediates inhibition and promotion of photosynthesis-related proteins

Proteomics analysis revealed a significant downregulation of Psb and Pet proteins in PSI, which subsequently reduced photosynthetic capacity. Conversely, photosystem II (44 kDa) and oxygen-evolved enhancer proteins were up-regulated in the PSII process. After 7 days of UV-B exposure, upregulation of the Hypersensitive to High Light1 protein and the psi-psb27 complex was detected, whereas the oxygen-united enhancer protein was down-regulated in membrane activity regulation. In addition, KEGG analysis revealed high enrichment of photosynthetic pathway proteins, 7 days following UV-B exposure . This indicated that UV-B mediates down-regulation of light reaction processes. However, upregulation of the photo-repair pathway demonstrated that UV-B may both inhibit and promote photosynthesis (Fig. 6).

### UV-B induces expression of resistance-related proteins

Proteomics analysis revealed that UV-B exposure mediated significant upregulation of the proteins involved in the antioxidant process. Specifically, phosphoethyl pyrimidine synthase was down-regulated in the chloroplasts, whereas degradation of aromatic compounds was up-regulated. Similarly, probable L-ascorbate peroxidase 6 (chloroplastic isoform X1) was significantly up-regulated at 7days of exposure. Specifically, a total of 18 and 11 proteins were significantly up- down-regulated, respectively 3 days post exposure. On the other hand, 17 and 4 proteins were significantly up-and down-regulated after 7 days of exposure. The significantly up-regulated proteins included oxidases or peroxidases, such as the protein DMR6-like oxygenase 2, geraniol 8-hydroxylase, probable mannitol dehydrogenase, cationic peroxidase, and cytochrome-related proteins (Table 4). Additionally, differentially expressed genes following KEGG enrichment analysis showed highly enrichment of antioxidant and repair pathways Table 5 .

**Table 4.** GO enrichment reveals profiles of gene expression

| Pair Comparison | GO accession | Description | Number of Up regulated genes | Number of down regulated genes |
|---|---|---|---|---|
| 3-day vs 0day | GO:0006338 | chromatin remodeling | 4 | 1 |
| | GO:0016491 | oxidoreductase activity | 18 | 11 |
| | GO:0006336 | DNA replication-independent nucleosome assembly | 1 | 1 |
| | GO:00031055 | chromatin remodeling at centromere | 1 | 1 |
| 7-day vs 0day | GO:0009512 | cytochrome b6f complex | 2 | 0 |
| | GO:0004474 | malate synthase activity | 1 | 0 |
| | GO:0006097 | glyoxylate cycle | 1 | 0 |
| | GO:0046487 | glyoxylate metabolic process | 1 | 0 |
| | GO:0019685 | photosynthesis, dark reaction | 1 | 0 |
| 3-day vs 7-day | GO:0001871 | pattern binding | 0 | 17 |
| | GO:0030247 | polysaccharide binding | 0 | 17 |
| | GO:0030246 | carbohydrate binding | 0 | 17 |

Note: Pathway significance enrichment analysis was conducted using the KEGG database, and adopted the hypergeometric test for identification of the pathway with significant enrichment in differentially expressed genes compared with that of the whole genome background. The calculation formula is as follows:

$$p=1-\sum_{i=0}^{m-1}\frac{\binom{M}{i}\binom{N-M}{n-i}}{\binom{N}{n}}$$

Where N is the number of genes with pathway annotation, n is the number of differentially expressed genes in N, M is the number of genes annotated as a particular pathway in all genes and m is the number of differentially expressed genes annotated as a particular pathway. FDR 0.05 indicated significant enrichment of differentially expressed genes in the related pathway, whereas KOBAS (2.0) was used for pathway enrichment analysis.

**Table 5.** Outline of differentially expressed genes following KEGG enrichment analysis

| Pair comparison | Pathway | Sample number | Background number | Corrected P-Value |
|---|---|---|---|---|
| 3-day vs 0day | Protein processing in endoplasmic reticulum | 7 | 222 | 0.01963777658 |
| 7-day vs 0day | Sesquiterpenoid and triterpenoid biosynthesis | 2 | 30 | 0.050938191 |
| 3-day vs 7-day | Circadian rhythm - plant | 7 | 74 | 0.0038186 |
| 3-day vs 7-day | Plant hormone signal transduction | 11 | 276 | 0.020775765 |
| 3-day vs 7-day | Flavonoid biosynthesis | 6 | 88 | 0.020775765 |

Note: The most significantly enriched KEGG pathways were selected. Term: descriptive information of KEGG pathway. Database: KEGG. ID: unique numbering information of the access in KEGG database. (4) Sample number: the number of differentially expressed genes in this pathway. Background number: the number of annotated genes in this pathway. Corrected p-value: the statistic significant level after correction. When the Corrected p-value is less than 0.05, the Corrected p-value becomes the accumulation item.

### Cell morphology-related pathways were significantly up-regulated following UV-B exposure

Analysis of metabolic pathways involved in cell morphology revealed a significant upregulation of proteins associated with cell morphology and cell wall synthesis (Table 6). The most enriched pathways were those involved in Linoleic acid metabolism, Isoquinoline alkaloid biosynthesis, and Gap Junction as well as proteins for the Tubulin beta-5, tubulin beta-1, and tubulin alpha-3 chains, and Polyphenol oxidase.

**Table 6.** Pathways involved in cell morphology

| Pair comparison | Pathways | Proteins |
|---|---|---|
| 3-day vs CK | Isoquinoline alkaloid biosynthesis | Polyphenol oxidase, chloroplastic-like[Vitis vinifera] |
| | Tyrosine metabolism | Polyphenol oxidase, chloroplastic-like [Vitis vinifera] |
| 7-day vs CK | Linoleic acid metabolism | Lipoxygenase [Vitis vinifera] |
| 3-day vs 7-day | Starch and sucrose metabolism | Cell wall apoplastic invertase [Vitis vinifera] |
| | Linoleic acid metabolism | Lipoxygenase 6, chloroplastic [Vitis vinifera] |
| | Phagosome | Tubulin beta-1 chain [Vitis vinifera] |
| | Gap Junction | Tubulin beta-1 chain [Vitis vinifera] |
| | Gap junction | Tubulin beta-5 chain, tubulin beta-1chain, tubulin alpha-3 chain [Vitis vinifera] |
| | Pathogenic Escherichia coli infection | Tubulin beta-5 chain, tubulin beta-1chain, tubulin alpha-3 chain [Vitis vinifera] |
| | Apoptosis | tubulin alpha-3 chain [Vitis vinifera] |

### Relationship between protein and gene expression across different UV-B exposuretreatments

Correlation analyses revealed high enrichment of genes and proteins involved in catalytic and metabolic processes (Fig.7 a-b). These results were obtained after analyzing data via http://wego.genomics.org.cn. Summarily, transcriptomic results were higher than proteomics for cellular component, molecular function and biological processes. Particularly, five GO enrichments, including metabolic processes and those related to membrane and catalytic activity, were over-represented. A resultant heatmap revealed that nearly 2/3 of regulations were over-expressed 3 days post exposure, with the remaining 1/3

restrained, owing to the fact that proteins tended to have low or no expression. In addition, proteins were upregulated when leaf samples were exposed for more than 3 days, whereas the others tended to have flat or no expression (Fig 7. c-e). In the present study, the selection criteria included (1) Fold changes of expression >2 in two group comparison, (2) *t*-test $p < 0.05$ and (3) at least three biological replicates.

### Validation of DEGs via real time PCR

To validate expression of the RNA-Seq data, we selected 10 genes across each of the identified DEG categories following RNA-Seq analysis, and used them for quantitative real time PCR. Results revealed that expression profiles of 7 genes involved in metabolism, antioxidant processes and defense responses were comparable with RNA-Seq results (Appendix Figure B1). This affirmed reliability of the transcriptome data.

## Discussion

A network of protein-protein interaction revealed significantly superior number of upregulated than downregulated proteins after 3 days of exposure (Fig. 5). In contrast, 7-day exposure resulted in a near similar up- and down-regulation of proteins as well as the Ascorbate metabolism and Dioxin degradation pathways. In addition, we detected, for the first time, enrichment of glyceraldehyde-3-phosphate dehydrogenase, cytosolic protein, ABC transporter B family member 11, cytochrome P450 84A1, ATP-dependent 6-phosphofructokinase 5, AAA-ATPase At3g50940-like protein and trans-cinnamate 4-monooxygenase pathways 3days after UV-B exposure. An increase in exposure time, to 7days, resulted in significant upregulation of the luminal-binding, and endoplasmin homolog proteins, as well as other unidentified ones. A comparison between 3 and 7-day exposure times revealed that the protein aldehyde dehydrogenase family 3 member H1 isoform X1, 3-hydroxyisobutyryl-CoA hydrolase-like protein 5, and 40S ribosomal protein S9-2, were involved in multiple metabolic pathways and biological processes as evidenced by big nodes in Fig.5-c.

### UV-B exposure mediated upregulation of cell wall synthesis and cytoskeleton-related proteins

in the present study, our proteomic results revealed significant upregulation of leaf epidermal and palisade tissue cells following exposure to UVB, which subsequently resulted in changes in cell morphology. Previous studies have reported significant upregulation of proteins and pathways associated with cell morphology and cytoskeleton. For example, xyloglucan endotransglucosylase was implicated in tomato and apple fruit ripening via loosening of cell wall11. Results of the present study showed a significant up-regulation of xyloglucan endotransglucosylase in wine grape leaves, which subsequently induced morphological changes, 3 days after UV-B exposure. Similarly, the Receptor protein kinase, TMK1, which has previously been implicated in auxin signal transduction, cell expansion and proliferation regulation12, was down-regulated after 3 days of UV-B exposure. This may indicate that TMK1 has a potential role in induction of changes in cell morphology of palisade tissue. Additionally, we also detected downregulation of NP_001267891.1 a protein known as the basic endochitinase precursor in Vitis vinifera, in cell wall macromolecule catabolic process (GO: 0016998). Previous studies have

shown that basic endochitinase precursor participates in polyphenol synthesis13, although only a handful of reports have associated it in cell wall macromolecule catabolic process. In the present study, we identified proteins involved in structural constituent of cytoskeleton and microtubules, and these were derived from the tubulin beta chain and tubulin alpha chain. GO enrichment (GO: 0005200) revealed significant downregulation of beta-tubulin across 3 and 7 days post exposure, with no significant differences between day 3 and 0. The Cytoskeleton is a complex that plays an important role in cell movement, shape formation and mechanical properties. In fact, Structural information on the cytoskeletal tissue is critical to understanding its functions and mechanisms across various forms of cellular activity14. In the present study, we found overexpression of the lipoxygenase (LXOA) in cytoskeletal tissue and detected its involvement in morphogenesis, cell wall formation, cellular development, and external encapsulating structure processes 7 days after UV-B exposure. Previous studies, targeting LXOA, have demonstrated that a lipoxygenase located inside the chloroplasts of tobacco leaves was able to catalyze membrane galactolipid peroxidation15. Moreover, our transcriptomic data revealed that activation of lipoxygenase after irradiation continued over a certain period of time, its enrichment in cell structure and morphological changes, as well as peroxidation within leaf epidermis. Similar responses were previously reported in the cell wall apoplastic invertase of Vitis vinifera, following UV-B irradiation treatment, in response to wounding, as well as powdery and downy mildew infection, suggesting a potential generalized response to stress16.

### Continuous UV-B treatment causes leaf chlorosis and increases stress resistance in plants

In the present study, the observed yellowing of leaves, under irradiation, might have been due to expression of 4 proteins, including probable zinc metallopeptidase EGY3, psbP domain-containing protein 1, and probable carotenoid cleavage dioxygenase 4 CCD4). These proteins have been previously shown to play important roles in yellowing of peach fruit. Moreover, downregulation of CCD4 in potato tubers was associated with yellowing of chrysanthemum flower[17,18]. Our correlation analysis showed a significant expression of the putative receptor-like protein kinase, At3g47110, between 3 and 7 days post exposure, as well as a significant increase in the role of catalytic activity in plant-pathogen interaction. This kinase is one of the Receptor-like protein kinase (RLKs), derived from a large multi-gene family in plants. In fact, at least 610 and 1131 members have been discovered in *Arabidopsis* and rice, respectively. Functionally, RLKs participate in a diverse range of processes, which can be divided into two broad categories. The first category comprises plant growth and development under normal growth conditions (0-day), whereas the second relates to disease resistance and stress responses[19]. Once a plant is subjected to environmental pressure, some RLK genes are enriched in signal transduction processes. Our results revealed upregulation of At3g47110 when plants were exposed to 20w/$m^2$ UV-B stress. This protein, previously discovered in both *Arabidopsis* and *Vitis vinifera*[20,21], may indicate activation of the second category of stress response of RLK as well as related gene-like 100259715. Notably, an additional Leaf rust 10 disease -resistance locus receptor-like protein kinase-like 1.2 isoform X1 and the Receptor protein kinase TMK1-like were also detected, and these have been previously found to be upregulated following attack by wheat rust pathogens upon induction of abiotic stress[22]. We hypothesize that a series

of stress responses may have enhanced the resistance to the invasion of pathogens under abiotic stress. Therefore, the TMK1-like protein probably contributes to selective response to diverse extracellular signals, such as the light stimulation. Furthermore, previous studies have shown that heat shock proteins like Hsp90 are essential regulators of cellular protein quality under normal conditions, and are involved in broad roles in protein folding, trafficking, and degradation[23,24]. In the present study, we observed a significant enrichment of metabolic, phosphorylation and serine -threonine, process following UV-B radiation, which may trigger the interaction between the heat shock protein and the TPR co-chaperones[25]. Besides, previous evidences suggest that certain viruses regulate the serine–threonine protein kinase (Known as PKR) activity via recruitment of a cellular stress pathway. For example, PKR was found to be a critical component for host defense response against viral infection[26], as well as a regulator of the NF-kB signal transduction pathway in our previous study[27]. Proteomic results revealed PKR activation in response to abiotic stress like UV-B irradiation, and may have been involved in signal transduction, although further studies are needed to verify this. Meanwhile the GRIP28, known as the ripening-related protein, was down-regulated after 3 days of treatment, indicating that it may be playing a role in cell wall structure/metabolism[28].

### Photosynthesis-related metabolic pathways are significantly enriched following UV-B exposure

We determined UV-B-induced photosynthetic changes at both transcriptomic and proteomic levels, and found that the photosystem II 44 kDa protein and the oxygen-evolving enhancer protein contributed to PS II (Photosynthetic system II), as well as photosystem II repair protein PSB27-H1 in the same pathway in the chloroplast (https://www.uniprot.org/uniprot/Q9LR64). In addition, prolonged irradiation resulted in differential expression of the Hypersensitive to High Light1 protein (HHL1). Previous studies on land plants have implicated this stroma-exposed thylakoid membrane located protein, associated with the PSII core monomer complex through direct interaction with the PSII core proteins CP43 and CP47, in repair and reassembly cycle of the PSII- under high-light conditions[29]. In addition, analysis of the psi-psb27 complex during the repair cycle after PSII inactivated under the light pressure, revealed that it is essential for survival of the cells under specific stress conditions[30]. Moreover, prolonged exposure times, from 3 to 7 days, resulted in detection of dynamic changes in the Antenna protein process of chlorophyll binding. This potentially shows activation of the Photosynthesis - antenna proteins embedded in the thylakoid membrane of plants, for enhanced energy capture and were capable of transferring light energy to one chlorophyll at the reaction center of photosystem[31]. Therefore, the Photosynthesis - antenna proteins together with the photosystem II repair protein PSB27-H1, may enhance resistance to light stress. Furthermore, the other two proteins, the oxygen-evolving enhancer protein 3 and 2, were significantly down-regulated in membrane activity. Functionally, these two chloroplast proteins specifically interact with the cytoplasmic kinase, and get phosphorylated in an AtGRP-3-dependent manner[32,33], to help mediate the arrangement of cell wall and signal transduction.

### UV-B treatment initiated a significant antioxidant process

Our results revealed specific enrichment of antioxidant processes at both molecular and cellular levels. Specifically, we found significant downregulation of Phosphomethyl pyrimidine synthase in the chloroplast, as well as expression of the pathway for degradation of aromatic compounds. Three proteins, key among them the one involved in Trans - cinnamate 4 - monooxygenase synthesis, were involved. Previous studies have shown that down-regulation of poly ADP-ribose polymerase (PARP) activity results in enhance resistance to abiotic stresses, such as temperature, excessive light and drought[34]. This factor has also been implicated in DNA repairing when irradiation damage reached a certain level[35]. In addition, XP_002285865.1, known as the probable L-ascorbate peroxidase 6, chloroplastic isoform X1, has been found to have a well-established intra-protoplasmic role as an antioxidant in chloroplasts[36]. For example, it was involved in response to abiotic stress (https://www.uniprot.org/uniprot/Q69SV0), with other studies hypothesizing that chloroplast morphology may be affected under illumination[37]. Ascorbate concentrations were considered a responsive signal coordinating activity of defense networks complementary to the antioxidant. Functionally, L-ascorbate oxidase Ascorbate was reported to play a key role in defense against oxidative-stress, and was particularly abundant in photosynthetic tissues of *Vitis vinifera* [38]. was Additional evidence has shown that ascorbate oxidase activity affects light acclimation, in which the lipid remodeling contributes to leaf acclimation also influenced by the AO activity. These studies indicate that Ascorbate biosynthesis and accumulation are regulated by the quantity and quality of incident light, such as UV-B in our study [39]. Additionally, photomorphogenic factors and UV-B receptors, such as UVR1, and Elongated Hypocotyl5 have previously been analyzed at the molecular level [40]. Our results reveal up-regulation of UVR1 and EH5 proteins in a widely adaptive species like winegrape, which are comparable to previously reported *Arabidopsis thaliana*, as well as E3 ubiquitin-protein ligase HERC1-like overexpressed in response to UV-B in *Cabinent Sauvignon*. Particularly, we identified 17 proteins involved in the oxidation-reduction process between 3 and 0-day samples. These genes were the most across all detected biological activities, , with 18 and 11 up- and down-regulated genes, respectively. A comparison between 7- and 0-day timepoints, revealed 17 and 4 up- and downregulated proteins, respectively. Increase in exposure time led to upregulation of oxygenase or peroxidases, such as the protein DMR6-like oxygenase 2, geraniol 8-hydroxylase, probable mannitol dehydrogenase, cationic peroxidase and cytochrome-related proteins. Among these, DMR6 plays a role in plant defense processes, and is activated following a biological infection[41]. From our results, it is evident that an increase in UV-B radiation initiated DMR6's involvement in coding defense proteins and regulating expression of related genes. A comparison between samples at 3 and 7 days of UV-B exposure revealed a significant different in expression of three genes. In addition, heavy metal-associated isoprenylated plant protein 9, peroxidase 64, and peroxidase P7 were significantly up-regulated in response to oxidative stress. Moreover, the sulfate transmembrane transport process was active in samples from both 3- and 7-day exposure groups, whereas 5'-adenylylsulfate reductase 3, chloroplastic protein was up-regulated in antioxidant activity following radiation. Previous studies have considered 5'-adenylylsulfate (APS) reductase a major 0-day part of sulfate metabolism owing to its accumulation in plants exposed to toxic stress[42]. According to this evidence, abiotic stresses, such as UV-B radiation, may induce enrichment of APS in sulfate-relay bioprocess. A comparison

between samples exposed to 7 days of UV-B radiation, with those under normal conditions (0-day), revealed downregulation of more proteins with increase in irradiation. On another hand, dynamic changes were observed in the pathway for Sulfur relay system, as well as mitochondrial activity and related enzymes. These findings indicated that the sulfur-relevant bioprocess was strengthened with prolonged UV-B exposure.

# Conclusions

Our results revealed significant cellular and molecular changes in epidermal and palisade cells of *Cabinent Sauvignon* plants exposed to 20w/$m^2$ UV-B for 3 and 7 days. Morphologically, 20w/$m^2$ UV-B resulted in shorter palisade tissue and epidermal cells, making them to be tightly packed. On the other hand, proteomics and transcriptomic analyses revealed significant upregulation of factors regulating oxidation process, photosynthesis, protein phosphorylation, cytoskeleton and microtubule formation processes following UV-B exposure. In addition, a short exposure to UV-B (no more than 7 days) enhanced photosynthetic ability, and induced expression of some resistance genes under abiotic stress. A combination of cellular, morphological and structural changes, with variations in biological processes, tend to enhance a plant's ability to resist abiotic stress.

# Methods

### Plant materials, growth conditions and light sources

The Cabinent Sauvignon plants grown for eight years in Yunnan were chosen as experimental materials. In order to ensure consistent test condition, eighteen plants with consistent growth were selected as experimental materials. Each plant maintains 5 to 7 branches, and main stems of each plant were kept at 1250mm high. Selected plants were transplanted into pots which were 260mm in height and 370mm in diameter. Each pot contains vermiculite, red soil, and humus, of which the proportion of soil was 1:1:3. We placed Eighteen pots in a glasshouse where temperature and humidity were 0-dayled (day and night temperature were 25/18℃ relatively humidity was 40%). In consideration of meeting the environmental conditions of the local wine grape regions as much as possible, we carried out meteorological monitoring on three major wine grape regions in Yunnan province and took the meteorological data of recent three years as a reference (2015-2017), found that the annual average UV-B radiation intensity was in between10-15w/$m^2$. The strongest UV-B intensity in the daytime was 22w/ $m^2$ (data was collected from the local meteorological database). The Lights were supplied by Photoelectric Instrument Factory of Beijing Normal University, Beijing, China (Philips. 20w/$m^2$, 6lamp tubes).

We set up three experimental groups with total 18plants, one 0-day group (CK) and two treatment groups. Each group contains 2lamps, 3 pots as three replicates (6plants of Cabinent Sauvignon). According to preliminary work, the phenotype appeared after 3-day irradiation; thereby in later experiment the duration of UV-B treatment was justified to 3 days and 7 days. The experiment was conducted from 10:00 am to 14:00 pm each day after dormant plants began to sprout and each branch has 5-6 leaves. In order to

ensure the consistency of measurement time, the 7-day exposure group was carried out 4 days in advance. One-thirds of the new leaves and developing leaves including the meristem were directly exposed to light (as described in Fig.8). The radiation intensity was measured by Hand-hold UV irradiation meter (Mode type: LS126. Manufacture: Linshang Technology. Co, Shenzhen, China. Measuring range of wavelength is 380nm-760nm). When plants get perpendicular to the tube, and were 10-15cm away from the lamp, the instant exposure intensity was around 3.8w/$m^2$. When the distance between the tube and the plants increased to 30-40cm, the exposure intensity decreased to 2.7-2.5w/$m^2$. The longer the distance was, the weaker the radiation would be. Every two pots of plants under each lamp were adjusted continuously during the test to ensure the evenness of light exposure.

## Anatomical observation and photosynthetic index determination

The leaves completely exposure to UV-B but capable of function were selected for anatomic and transcriptomic analysis. Among which, 3-5 leaves from each plant were cut into small pieces in the size of 5mmx5mm then put into the pre-configured glutaraldehyde fixer for one week. All samples were cleaned, embedded with resin for slicing. Each embedded section was cut into 5μm thick slice by the Leica EM UC7 ultra-thin slicer (manufacture Germany) for observation under 20-fold microscope. We performed photosynthetic measurement on three groups from 10:00 am every hour until 2:00 pm on the third and seventh day of exposure[43].

## Proteomic materials and methods

## Sample collection

The TMT (Tandem Mass Tags) technology innovated by Thermo SCIENTIFIC. Co. USA, was used to measure the expression level of proteins. Samples were gathered right after lights off from treated plant treated for 3 days exposure time was 12 hours , so did the 7-day treatment group. For the untreated samples, we collected samples for three times: 0day, 3 days and 7 days; collecting time was consistent with the treatment groups. A total of leaves of the same size were selected, stored in liquid nitrogen then delivered to Novogene technology Co. (Beijing, China) for proteomic and transcriptomic analysis.

## Total protein extract

The samples were individually milled to a power in a mortar with liquid nitrogen then mixed 150 mg of the powder from each sample with 1 ml of lysis buffer containing Tris-base (pH 8), 8M Urea, 1% SDS, complete protease inhibitor cocktail (Sigma) in a glass homogenizer. The homogenate was incubated on ice for 20 min and then centrifuged at 12000 g for 15 min at 4°C and protein concentration was determined with a Bradford assay. Then 4 volumes 10 mM DTT were added in cold acetone to a sample extract, Vortexed well, placed sample at -20°Cfor 2 h to overnight. Centrifuged and collected pellet to wash twice with cold acetone. Finally dissolve the pellet by dissolution buffer containing Tris-base (pH=8), 8M Urea.

## Peptide preparation

The supernatant from each sample, containing precisely 0.1mg of protein, DTT reduction,

iodoacetamide alkylation, and was digested with Trypsin Gold (Promega, Madison, WI) at 37°C for 16h. After trypsin digestion, peptide was desalted with C18 cartridge to remove the high urea, and desalted peptides were dried by vacuum centrifugation.

## TMT labeling of peptides

Desalted peptides were labeled with TMT10-plex reagents (TMT10plex™ Isobaric Label Reagent

Set, Thermofisher), following the manufacturer's instructions. For 0.1mg of peptide, 1 unit of labeling reagent was used. Peptides were dissolved in 30µl of 0.1 M triethylammonium bicarbonate solution

(TEAB, pH 8.5), and the labeling reagent was added to 20µl of acetonitrile. After incubation for 1 h, the reaction was stopped with 50 mM Tris/HCl (pH 7.5). Differently labeled peptides were mixed equally and then desalted in 100 mg SCX columns (strata-x-c, Phenomenex: 8B-S029-EBJ).

## HPLC fractionation

A ~600 microgram TMT-labeled peptide mix was fractionated using a C18 column (waters BEH

C18 4.6 × 250 mm, 5 µm) on a Rigol L3000 HPLC operating at 1ml/min. The column oven was set

as 50 °C. Mobile phases A (2% acetonitrile, 20mM NH4FA, adjusted pH to 10.0 using NH3·H2O) and

B (98% acetonitrile, 20mM NH4FA, adjusted pH to 10.0 using NH3ÀH2O) were used to develop a

gradient elution. The solvent gradient was set as follows: 3–8% B, 5min; 8–18% B, 12 min; 18–32% B,

11 min; 32–45% B, 7 min; 45–80% B, 3 min; 80% B, 5 min; 80–5% 0.1min 5% B, 7 min The tryptic peptides were monitored at UV 214 nm. Eluent was collected every minute and then merged to 15 fractions. The samples were dried under vacuum and reconstituted in 20µl of 0.1% (v/v) FA, 3% (v/v) acetonitrile in water for subsequent analyses.

## LC-MS/MS analysis

Fractions from the first dimension RPLC were dissolved with loading buffer and then separated by a C18 column (150µm inner-diameter, 360µm outer-diameter×15cm, 1.9µm C18, Reprosil-AQ Pur, Dr. Maisch). Mobile phase A consisted of 0.1% formic acid in water solution, and mobile phase B consisted of 0.1% formic acid in acetonitrile solution; a series of adjusted 60mingradients according to the hydrophobicity of fractions eluted in 1D LC with a flow rate of 300 nL/min was applied. Q-Exactive HF-X mass spectrometer was operated in positive polarity mode with capillary temperature of 320°C.Full MS scan resolution was set to 60000 with AGC target value of 3e6 for a scan range of 350-1500m/z. A data-

dependent top 40 method was operated during which HCD spectra was obtained at 15000 MS2 resolution with AGC target of 1e5 and maximum IT of 45ms, 1.6 m/z isolation window, and NCE of 30, dynamically excluded of 60s.

### The identification and quantitation of protein

The resulting spectra from each fraction were searched by the search engines: Proteome Discoverer 2.2 (PD 2.2, Thermo). The searched parameters as follows: A mass tolerance of 10 ppm for precursor ion scans and a mass tolerance of 0.02 Da for the product ion scans were used. Carbamidomethyl was specified in PD 2.2 as fixed modifications. Oxidation of methionine, acetylation of the N-terminus and TMT 10-plex of lysine were specified in PD 2.2 as variable modifications. A maximum of 2 miscleavage sites were allowed. For protein identification, protein with at least 1 unique peptide was identified at FDR less than 1.0% on peptide and protein level, respectively. Proteins containing similar peptides and could not be distinguished based on MS/MS analysis were grouped separately as protein groups. Reporter Quantification (TMT 10-plex) was used for TMT quantification. The protein quantitation results were statistically analyzed by Mann-Whitney Test.

### Transcriptomic analysis

### Sample collection and preparation

### RNA quantification and qualification

RNA degradation and contamination were monitored on 1% agarose gels. RNA purity was checked using the NanoPhotometer® spectrophotometer (IMPLEN, CA, USA). RNA concentration was measured using Qubit® RNA Assay Kit in Qubit® 2.0 Flurometer (Life Technologies, CA, USA). RNA integrity was assessed using the RNA Nano 6000 Assay Kit of the Bioanalyzer 2100 system (Agilent Technologies, CA, USA).

### Library preparation for Transcriptome sequencing

A total amount of 1 μg RNA per sample was used as input material for the RNA sample preparations. Sequencing libraries were generated using NEBNext® UltraTM RNA Library Prep Kit for Illumina® (NEB, USA) following manufacturer's recommendations and index codes were added to attribute sequences to each sample. Briefly, mRNA was purified from total RNA using poly-T oligo-attached magnetic beads. Fragmentation was carried out using divalent cations under elevated temperature in NEBNext First Strand Synthesis Reaction Buffer(5X). First strand cDNA was synthesized using random hexamer primer and M-MuLV Reverse Transcriptase(RNase H-). Second strand cDNA synthesis was subsequently performed using DNA Polymerase I and RNase H. Remaining overhangs were converted into blunt ends via exonuclease/polymerase activities. After adenylation of 3' ends of DNA fragments, NEBNext Adaptor with hairpin loop structure were ligated to prepare for hybridization. In order to select cDNA fragments of preferentially 250~300 bp in length, the library fragments were purified with AMPure XP system (Beckman Coulter, Beverly, USA). Then 3 μl USER Enzyme (NEB, USA) was used with size-selected, adaptor-ligated cDNA at 37°C for 15 min followed by 5 min at 95 °C before PCR. Then PCR was

performed with Phusion High-Fidelity DNA polymerase, Universal PCR primers and Index (X) Primer. At last, PCR products were purified (AMPure XP system) and library quality was assessed on the Agilent Bioanalyzer 2100 system.

### Clustering and sequencing

The clustering of the index-coded samples was performed on a cBot Cluster Generation System using TruSeq PE Cluster Kit v3-cBot-HS (Illumia) according to the manufacturer's instructions. After cluster generation, the library preparations were sequenced on an Illumina Hiseq platform and 125 bp/150 bp paired-end reads were generated. Quality 0-day Raw data (raw reads) of fastq format were firstly processed through in-house perl scripts. In this step, clean data (clean reads) were obtained by removing reads containing adapter, reads containing ploy-N and low-quality reads from raw data. At the same time, Q20, Q30 and GC content the clean data were calculated. All the downstream analyses were based on the clean data with high quality.

### Data analysis

### Quality control

Raw data (raw reads) of fastq format were firstly processed through in-house perl scripts. In this step, clean data (clean reads) were obtained by removing reads containing adapter, reads containing ploy-N and low quality reads from raw data. At the same time, Q20, Q30 and GC content the clean data were calculated. All the downstream analyses were based on the clean data with high quality.

### Reads mapping to the reference genome

Reference genome and gene model annotation files were downloaded from genome website directly. Index of the reference genome was built using Hisat2 v2.0.4 and paired- end clean reads were aligned to the reference genome using Hisat2 v2.0.4. We selected Hisat2 as the mapping tool for that Hisat2 can generate a database of splice junctions based on the gene model annotation file and thus a better mapping result than other non-splice mapping tools.

### Quantification of gene expression level

HTSeq v0.9.1 was used to count the reads numbers mapped to each gene. And then FPKM of each gene was calculated based on the length of the gene and reads count mapped to this gene. FPKM, expected number of Fragments Per Kilobase of transcript sequence per Millions base pairs sequenced, considers the effect of sequencing depth and gene length for the reads count at the same time, and is currently the most commonly used method for estimating gene expression levels (Trapnell, Cole, et al., 2010).

### Differential expression analysis

Differential expression analysis of two conditions/groups (two biological replicates per condition) was performed using the DESeq R package (1.18.0). DESeq provide statistical routines for determining

differential expression in digital gene expression data using a model based on the negative binomial distribution. The resulting P-values were adjusted using the Benjamini and Hochberg's approach for 0-dayling the false discovery rate. Genes with an adjusted P-value <0.05 found by DESeq were assigned as differentially expressed[44,45].

### GO and KEGG enrichment analysis of differentially expressed genes

The GO enrichment analysis was performed of differentially expressed genes by the GOseq R package. The gene length bias was corrected. GO terms with corrected P-value less than 0.05 were considered significantly enriched by differential expressed genes. For KEGG analysis, we used KOBAS software to test the statistical enrichment of differential expression genes in KEGG pathways.

# Declarations

### Availability of data

The mass spectrometry proteomics data have been deposited to the ProteomeXchange Consortium via the PRIDE partner repository with the dataset identifier PXD013308.Transcriptome datasets can be retrieved from the NCBI SRA database of Project ID PRJNA528770, the wine grape leaf transcriptome.

### Acknowledgment

We thank Academician Zhu youyong and supervisor He xiahong for experimental guidance and article supervision; thank Xundian Practice base for providing experimental plants, Novogene.Co for technical assistance; the National engineering research center for agricultural biodiversity, Yunan Agircultural University for providing experimental platform; Mr. Wang, congde for help with section microscopy; Wang yi for supporting data analysis; and Zhu shusheng, Li chengyun for data review and writing guidance. This work was supported by grants from the Yunnan provincial science and technology department, Academician Free Exploration Project, grant number 2018HA009, and the Yunnan Provincial Administration of Foreign Experts Affair, Foreign Experts Introduction Project, grant number YNZ 2016006.

# References

1. Robinson, J. The Oxford Companion to Wine. (Oxford University Press, Oxford,1994).
2. Zhang J, Tian LP Research on plant growth treated with enhanced UV-B radiation. Chinese Agricultural Science Bulletin 25(22):104-108 (2009).
3. Sun Y ZW, et al. Enhanced effects of uv-b radiation on grape berries. Agricultural Research in the Arid Areas 28(1):164-167 (2010).
4. Basiouny, FM., Van, TK., Biggs, RH. (1978) Some morphological and biochemical characteristics of C3 and C4 plants irradiated with UV- B[J]. Physiol. Plant, 42:29-32.

5. Reyes TH, Scartazza A, Castagna A, et al. Physiological effects of short acute UVB treatments in Chenopodium quinoa Willd[J]. Scientific Reports, 2018, 8(1).
6. Clayton W A , Albert N W , Thrimawithana A H , et al. UVR8-mediated induction of flavonoid biosynthesis for UVB tolerance is conserved between the liverwort\r, Marchantia polymorpha\r, and flowering plants[J]. The Plant Journal, 2018.
7. Liu P , Li Q , Li Y , et al. Effect of UV-B radiation treatments on growth, physiology and antioxidant systems of cucumber seedlings in artificial climate chamber[J]. Nongye Gongcheng Xuebao/Transactions of the Chinese Society of Agricultural Engineering, 2017, 33(17):181-186.
8. Maria, Orodan & Morgovan, Claudiu & Olah, Neli-Kinga & Paul, Atyim & Toth, Csongor & Viorel, Orasan & Irina, Orasan & Gyongyi, Osser. (2015). Antioxidant system response on action of UVB radiation on plant systems. Analele Universităţii din Oradea, Fascicula: Ecotoxicologie, Zootehnie şi Tehnologii de Industrie Alimentară. XIV. 373-378.
9. Keller, Markus & Torres-Martinez, N.(2004). Does UV radiation affect winegrape composition?. Acta Horticulturae. 640. 313-319. 10.17660/ActaHortic.2004.640.36.
10. Luca R, Jean-Jacques, Favory, et al. Nogués Perception of UV-B by the Arabidopsis UVR8 Protein. Science 01 Apr: 103-106(2011).
11. Salvador Nogués, Damian J, Allen, et al. Ultraviolet-B Radiation Effects on Water Relations, Leaf Development, and Photosynthesis in Droughted Pea Plants. Plant Physiology May 117 (1): 173-181 (1998) .
12. Liu Yun, Zhang CZ. Differential response of leaf gas exchange to enhanced ultraviolet-B (UV-B) radiation in three species of herbaceous climbing plants. Acta Ecologica Sinica, Volumn29, Issue 2.124-129 (2009).
13. Sztatelman O, Grzyb J, et al. The effect of UV-B on Arabidopsis leaves depends on light conditions after treatment. BMC Plant Biol. 15:281 (2015).
14. Kobashigawa C, Tamaya K, et al. EFFECT OF UV-C TREATMENT ON PLANT GROWTH AND NUTRIENT CONTENTS. Acta Hortic 907, pp.237-242(2011).
15. Kanlaya Sripong, Pongphen Jitareerat, et al. UV irradiation induces resistance against fruit rot disease and improves the quality of harvested mangosteen. Postharvest Biology and Technology. Volume149: 187-194(2019).
16. Young MD, Wakefield MJ, et al. Gene ontology analysis for RNA-seq: accounting for selection bias. Genome Biol 11: R14 (2010).
17. Hauduc, Hélène, Johnson, et al. Incorporating Sulfur and Relevant Reactions into a General Plantwide and Sewer Model. IFAC-Papers on Line 50:3935-3940(2017).
18. J Muñoz-Bertomeu, E Miedes, et al Expression of xyloglucan endotransglucosylase/hydrolase (XTH) genes and XET activity in ethylene treated apple and tomato fruits, Journal of Plant Physiology. Volume170, Issue 13: 1194-1201(2013).
19. Perrot-Rechenmann C. Cellular responses to auxin: division versus expansion. Cold Spring Harb Perspect Biol 2(5): a001446(2010).

20. Da Silva C, Zamperin G, Ferrarini A, et al.The high polyphenol content of grapevine cultivar tannat berries is conferred primarily by genes that are not shared with the reference genome. Plant Cell 25(12): 4777-88(2013).
21. Svitkina T. Imaging Cytoskeleton Components by Electron Microscopy. Methods Mol Biol 1365:99-118 (2016).
22. Pilati S, Brazzale D, Guella G, et al. The onset of grapevine berry ripening is characterized by ROS accumulation and lipoxygenase-mediated membrane peroxidation in the skin. BMC Plant Biol 14:87(2014).
23. Hayes MA, Feechan A, Dry IB. Involvement of abscisic acid in the coordinated regulation of a stress-inducible hexose transporter (VvHT5) and a cell wall invertase in grapevine in response to biotrophic fungal infection. Plant Physiol 153(1):.211-21 (2010).
24. Justin G, Lashbrooke, Philip R, Young, et al. Functional characterisation of three members of the Vitis viniferaL. carotenoid cleavage dioxygenase gene family. BMC Plant Biology 13:156 (2013).
25. Rubab Zahra, Naqvi, Syed Shan-e-Ali Zaidi, et al. Transcriptomics reveals multiple resistance mechanisms against cotton leaf curl disease in a naturally immune cotton species, Gossypium arboreum. Scientific Reports 7:10.1038/s41598-017-15963-9(2017).
26. Shin-Han Shiu, Anthony B Bleecker. Plant Receptor-Like Kinase Gene Family: Diversity, Function, and Signaling. Science's STKE, Volume, 2001, Issue 113:re22 (2001).
27. Liang danna, Liu Min, et al. Identification of differentially expressed genes related to aphid resistance in cucumber (Cucumis sativus L.). Scientific reports 5:9645, 10.1038/srep09645 (2015).
28. Dang PM, Lamb MC, et al. Identification of expressed R-genes associated with leaf spot diseases in cultivated peanut. Mol Biol Rep 46:225(2019).
29. Cho hea-seong, S Pai H. Cloning and characterization of NtTMK1 gene encoding a TMK1-homologous receptor-like kinase in tobacco. Molecules and cells 10:317-24(2000).
30. Kundrat L, Regan L. Balance between folding and degradation for Hsp90-dependent client proteins: a key role for CHIP. Biochemistry 49:7428–7438(2010).
31. Young JC, Agashe VR, Siegers K, et al. Pathways of chaperone-mediated protein folding in the cytosol. Nat Rev Mol Cell Bio 5:781–791(2004).
32. Assimon VA, Southworth DR, Gestwicki JE. Specific Binding of Tetratricopeptide Repeat Proteins to Heat Shock Protein 70 (Hsp70) and Heat Shock Protein 90 (Hsp90) Is Regulated by Affinity and Phosphorylation. Biochemistry 54(48):7120-31(2015).
33. Gal-Ben-Ari S, Barrera I, Ehrlich M, et al. PKR: A Kinase to Remember. Front Mol Neurosci 11: 480(2019).
34. A Maran, RK Maitra, et al. Blockage of NF-kappa B signaling by selective ablation of an mRNA target by 2-5A antisense chimeras. Science, Volume, 265, Issue 5173: 789-792 (1994).
35. Davies C, Robinson SP. Differential screening indicates a dramatic change in mRNA profiles during grape berry ripening. Cloning and characterization of cDNAs encoding putative cell wall and stress

response proteins. Plant Physiol 122(3):803-12 (2000).

36. Jin HL, Liu B, et al. HYPERSENSITIVE TO HIGH LIGHT1 Interacts with LOW QUANTUM YIELD OF PHOTOSYSTEM II1 and Functions in Protection of Photosystem II from Photodamage in Arabidopsis. The Plant Cell Mar26 (3):1213-1229(2014).
37. Grasse Nicole, Mamedov Fikret, et al. Role of novel dimeric photosystem II (PSII)-Psb27 protein complex in PSII repair. The Journal of biological chemistry 286. 295:48-55(2011).
38. Guberman-Pfeffer M J, Gascón JA. Carotenoid-Chlorophyll Interactions in a Photosynthetic Antenna Protein: A Supramolecular QM/MM Approach. Molecules 23, 2589(2018).
39. Ju Y, Eun & Ah Oh, et al. Oxygen-evolving enhancer protein 2 is phosphorylated by glycine-rich protein 3/wall-associated kinase 1 in Arabidopsis. Biochemical and biophysical research communications: 305(2003).
40. Ae Ran P, Somi K Cho, et al. Interaction of the Arabidopsis Receptor Protein Kinase Wak1 with aGlycine-rich Protein, AtGRP-3. Journal of Biological Chemistry Volume, 276, No. 28: 26688 – 26693(2001).
41. Briggs AG, Bent AF. Poly (ADP-ribosyl) ation in plants. Trends. Plant Sci 16:372-380(2011).
42. M D'Arcangelo, Y Drew, R Plummer. The role of PARP in DNA repair and its therapeutic exploitation. DNA Repair in Cancer Therapy. Molecular Targets and Clinical Applications:115-134 (2016).
43. Foyer C H, Shigeoka S. Understanding oxidative stress and antioxidant functions to enhance photosynthesis. Plant Physiol 155: 93–100(2011).
44. Christine H Foyer, Graham Noctor. Redox Homeostasis and Antioxidant Signaling: A Metabolic Interface between Stress Perception and Physiological Responses. The Plant Cell Jul 17 (7): 1866-1875(2005) .
45. Pignocchi C, Fletcher JM, et al. The function of ascorbate oxidase in tobacco. Plant Physiol 132(3):1631-41 (2003).
46. Yabuta Y, Mieda.T, Rapolu M, et al. Light regulation of ascorbate biosynthesis is dependent on the photosynthetic electron transport chain but independent of sugars in Arabidopsis. J Exp Bot 58: 2661–2671(2007) .
47. Loyola R, Herrera D, Mas A, et al. The photomorphogenic factors UV-B RECEPTOR 1, ELONGATED HYPOCOTYL 5, and HY5 HOMOLOGUE are part of the UV-B signalling pathway in grapevine and mediate flavonol accumulation in response to the environment. J Exp Bot 67(18): 5429-5445(2016).
48. Van Damme, Mireille, et al. Arabidopsis DMR6 encodes a putative 2OG-Fe (II) oxygenase that is defense-associated but required for susceptibility to downy mildew. The Plant journal: for cell and molecular biology 54:785-93(2008).
49. Martin M N, Tarczynski M C, Shen B, et al. The role of 5'-adenylylsulfate reductase in 0-dayling sulfate reduction in plants. Photosynth Res 86:309-323 (2005).
50. Hellman Edward. Grapevine Structure and Function. Grape Grower's Handbook (2003).

51. Wang Z, M Gerstein, et al. RNA-Seq: a revolutionary tool for transcriptomics. Nature Reviews Genetics (2009).
52. Trapnell C, A Roberts, et al. Differential gene and transcript expression analysis of RNA-seq experiments with TopHat and Cufflinks. Nature protocols (2012).

# Figures

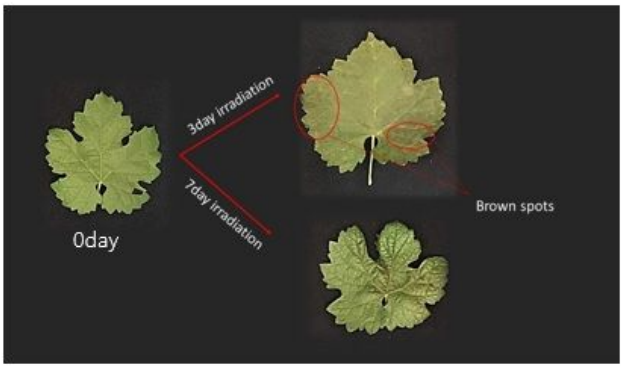


(a)

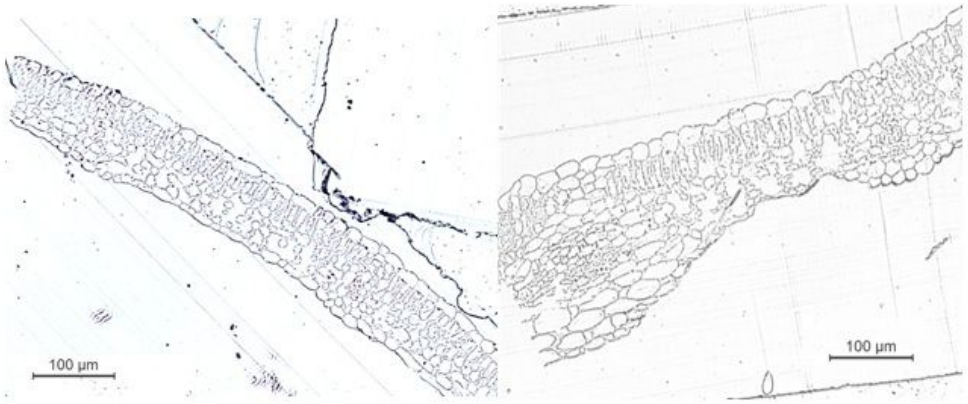


CK 3-day

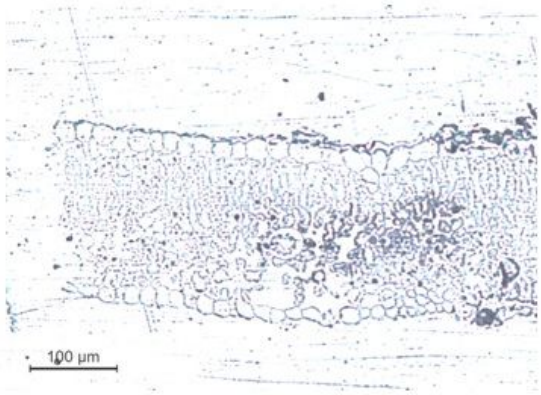


7-day

(b)

## Figure 1

Phenotypic changes in grape leaves following exposure to UV-B radiation. (a). Leaf apparent characteristics. (b). Transverse (upper panel) and paradermal sections (bottom panel) of new leaves emerging after exposure to UV-B. N=30, leaves with the most prominent characters were selected.

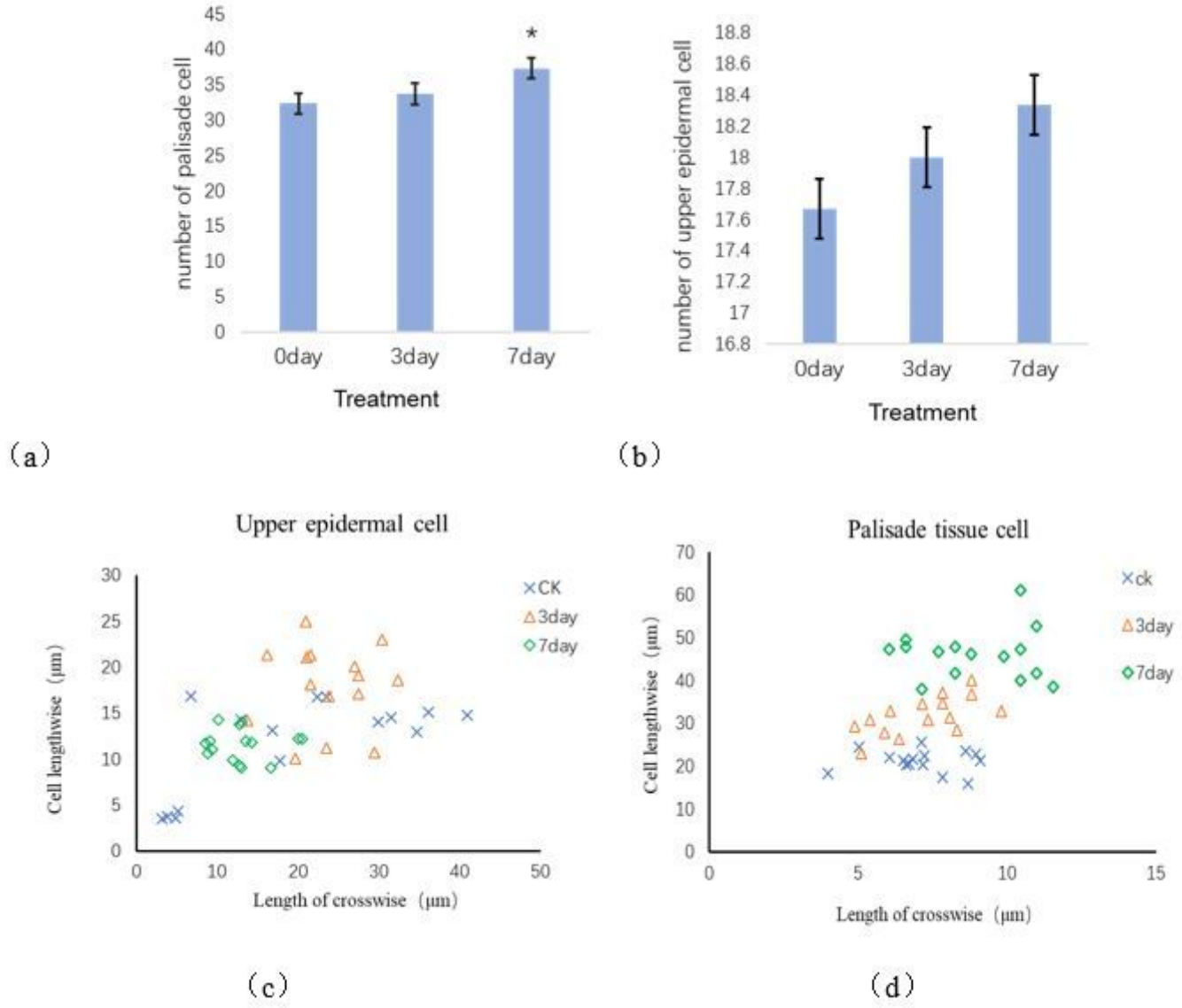


## Figure 2

Changes in morphological and density of palisade tissue and epidermal cells. (a) Cell density of palisade tissue per unit area (400x80 μm). (b) Cell density of epidermal cells in the same area (400x80 μm). (c) Scatter plot showing length of epidermal cells determined from transverse sections in each treatment. n = 60, Superscript '*' indicates significant difference $p<0.05$). d Scatter plot describing of epidermal cells. Leaves with a blade length of 25–35 mm were examined.

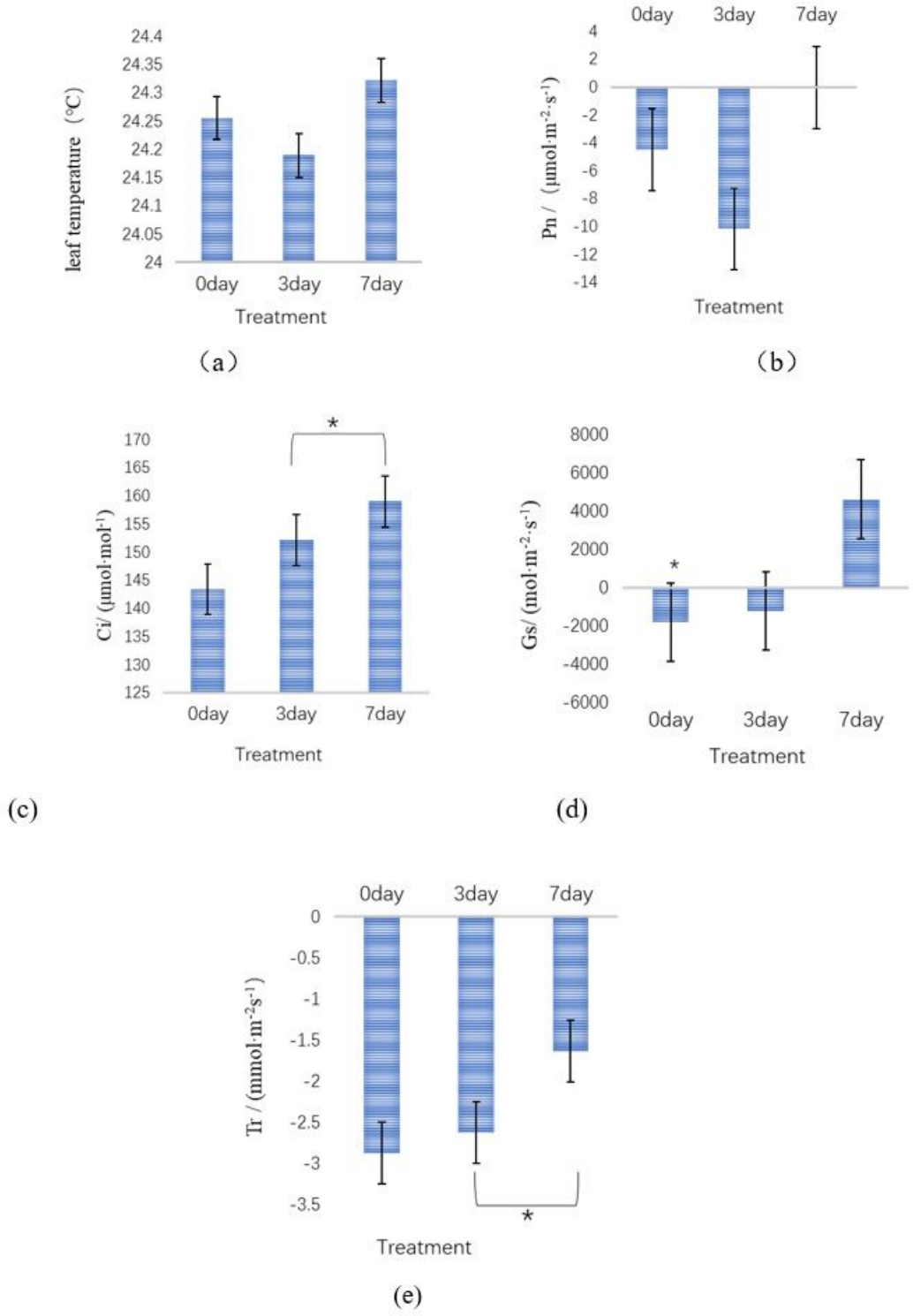


## Figure 3

Profiles of photosynthetic physiological indices after UV-B exposure. (a) Blade temperature. (b) Net photosynthetic rate. (c) Intercellular carbon dioxide concentration. (d) Leaf stomatal conductance. (e) Leaf transpiration rate. Superscript '*' indicates significant differences at P≤0.05 (N=60, P < 0.05).

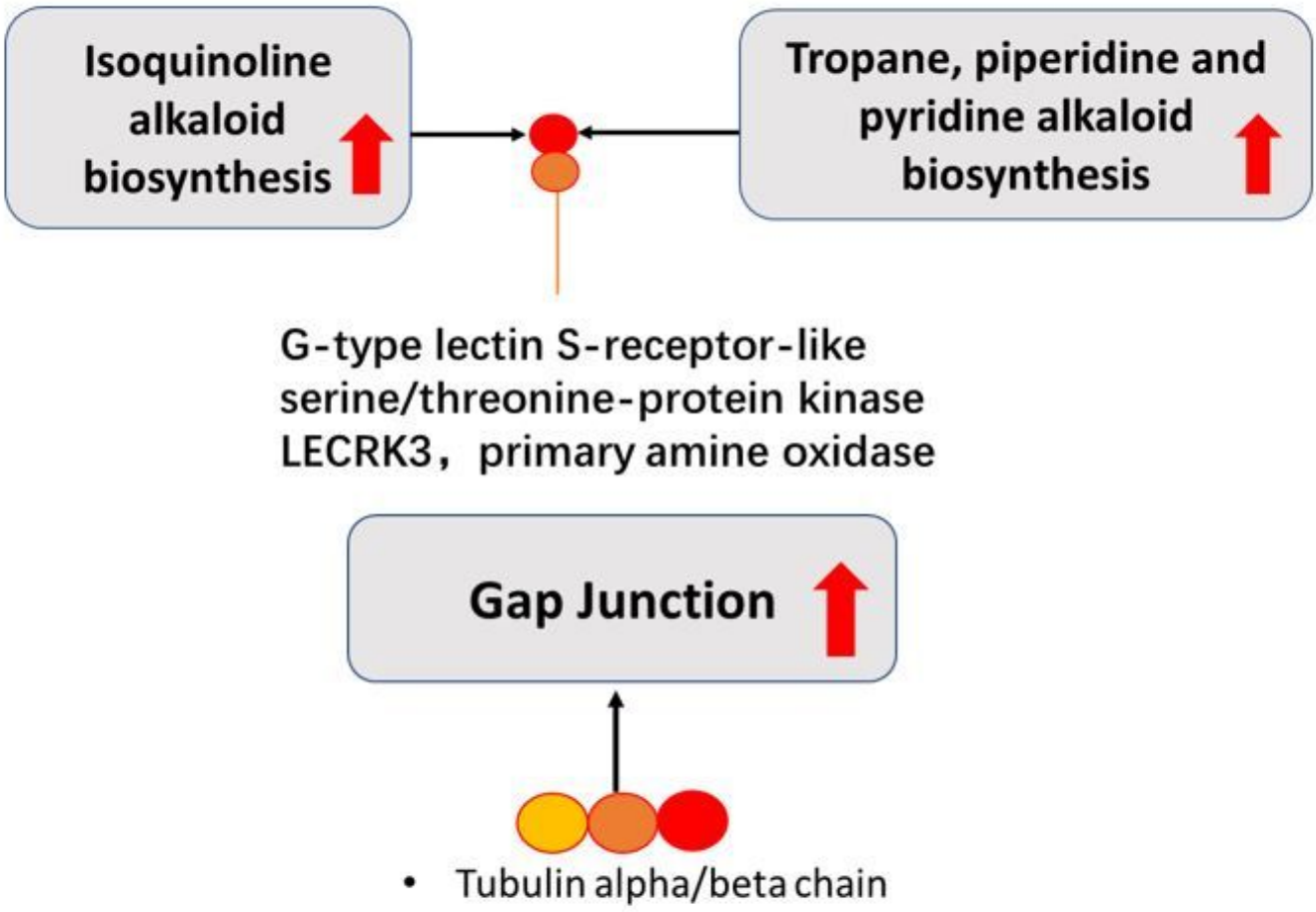


**Figure 4**

UV-B-induced upregulated proteins involved in cell morphological correlation pathway. The red arrow indicates up-regulation, whereas the circle denotes protein varieties.

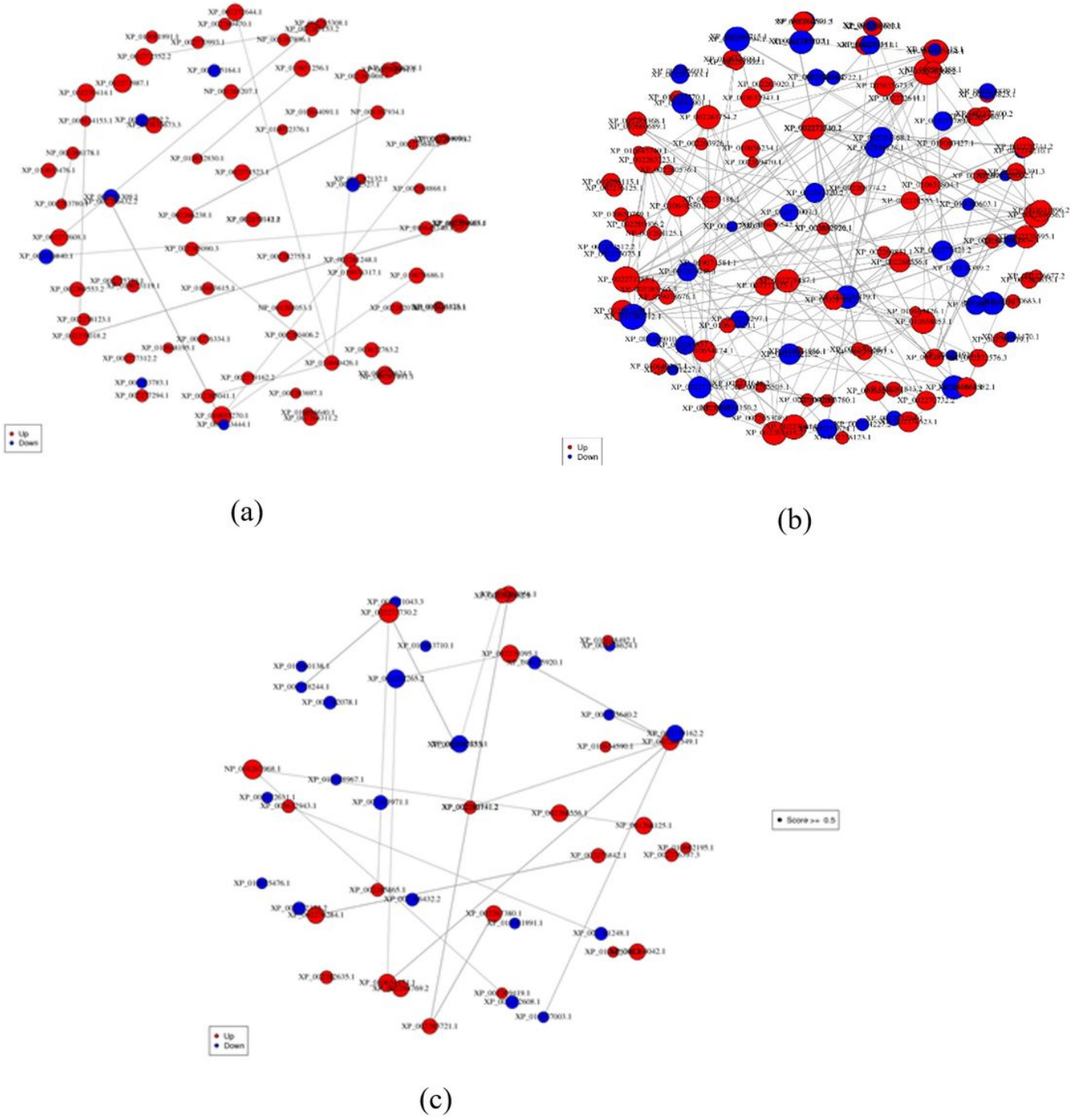


## Figure 5

Network analysis indicating Protein-protein interactions Node size in the interactive network is directly proportional to the degree of node. More lines connected to a node indicate how bid the node will be. (a) Highly up-regulated proteins can be seen in the 3-day group. (b) The number of downregulated proteins increased with increase in time (to 7 days). (c) A comparison across 3 and 7-day irradiation revealed a similar profile of up- and down-regulated proteins.

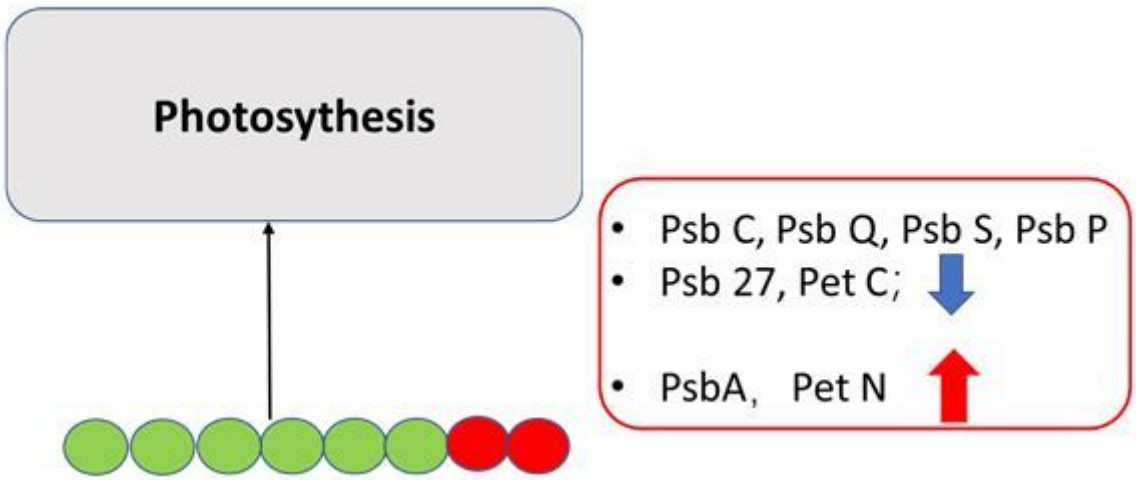


**Figure 6**

Expression profiles of proteins involved in the photosynthesis pathway. The red and blue arrows indicate up- and downregulation, respectively, whereas the circle denotes protein varieties

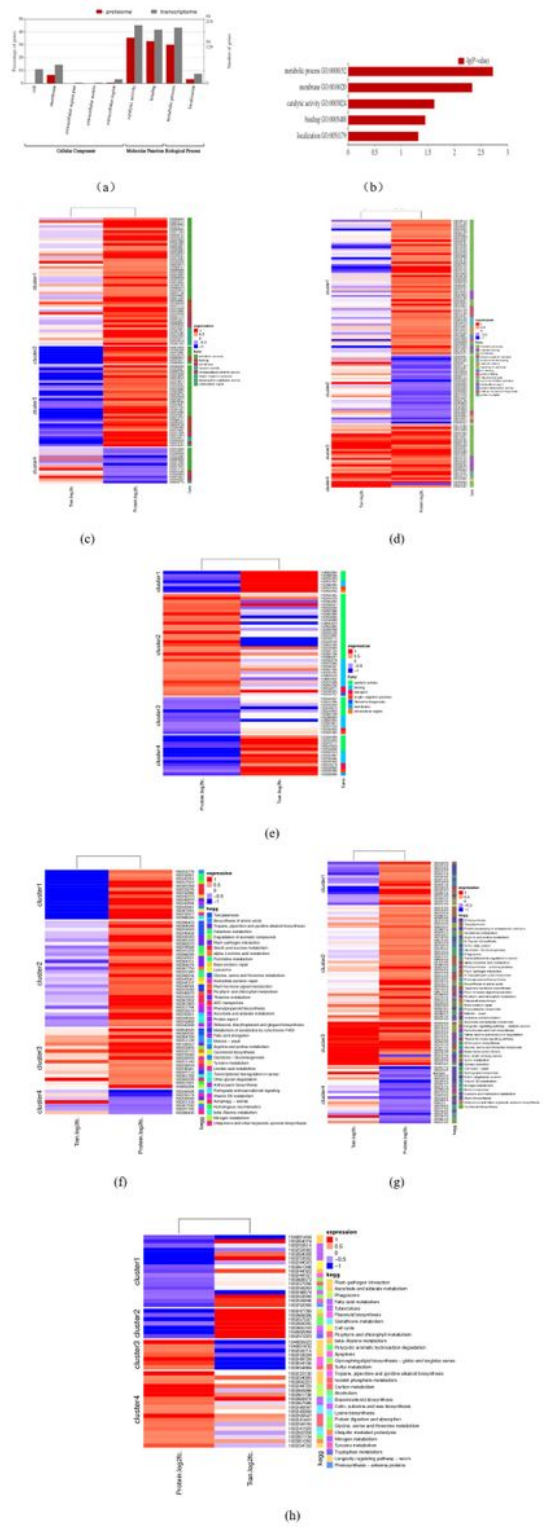

## Figure 7

Comparisons in changes Biological processes, cellular components and molecular function between groups. (a) The red and grey columns represent GO enrichment results for the proteome and transcriptome, respectively. The abscissa is the enriched GO entries, and the ordinate is the enriched genes of both proteome and transcriptome. (b) Significantly expressed metabolic pathways were identified following GO enrichment. (c) GO enrichment comparison between 3 and 0 days after exposure.

(d) Comparisons in GO enrichment between 7 and 0 days following exposure. (e) GO enrichment comparison between 3 and 7 days post exposure. (f) Comparisons in KEGG enrichment between 3 and 0 days after exposure. (g) Comparisons in KEGG enrichment between 7 and 0 days post exposure. (h) Comparisons in KEGG enrichment between 3 and 7 days. Red and blue denote up- and down-regulation, respectively. Horizontal clustering indicates profiles of protein expression at transcriptome and proteome levels, whereas the abscissa indicates functional classification. The ordinate is the number of proteins annotated to corresponding functions.

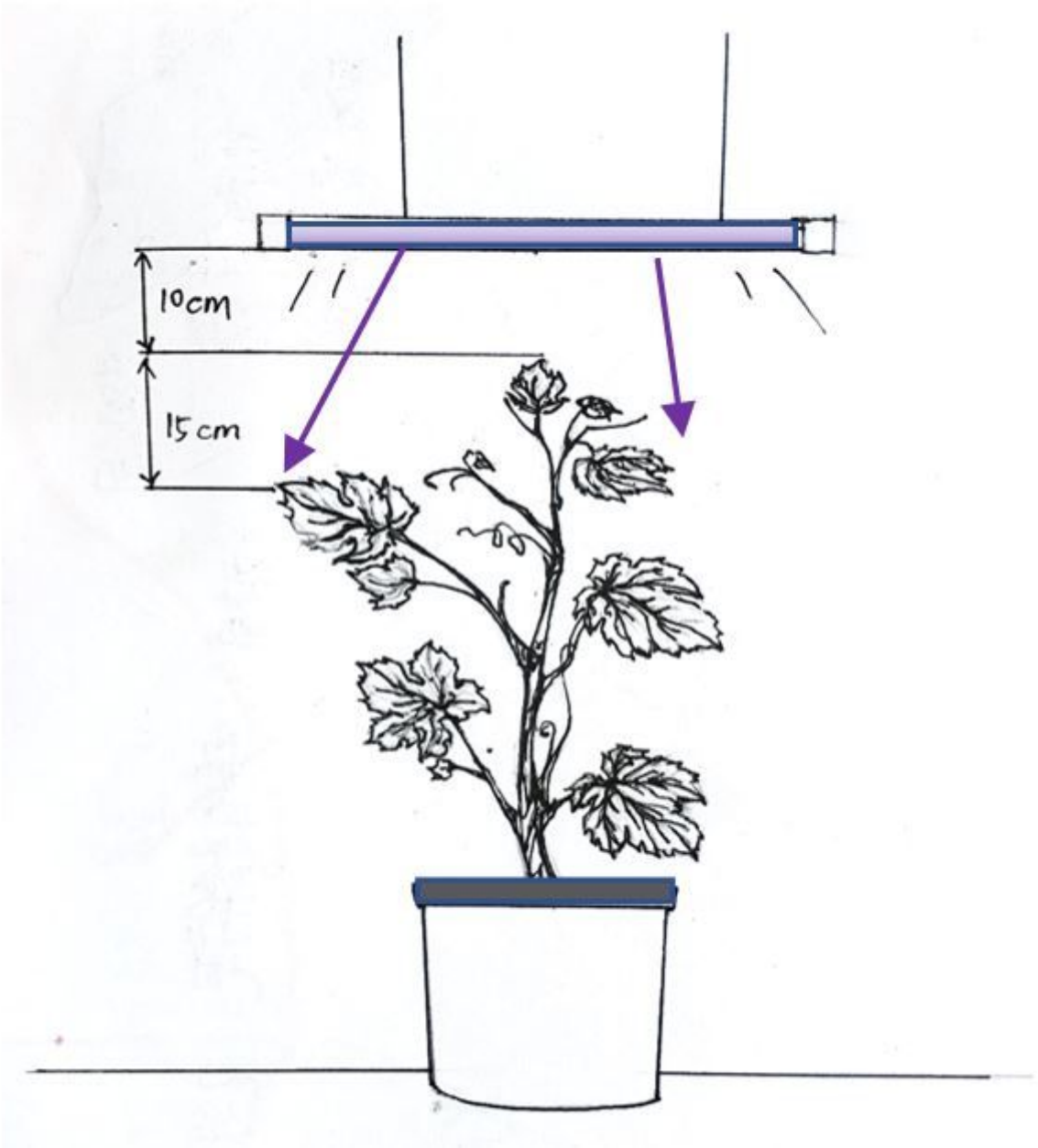


**Figure 8**

Potted wine grape irradiation experiment (Picture was drawn by author)

# Supplementary Files

This is a list of supplementary files associated with this preprint. Click to download.

- AdditionalInformation.docx